The College of Engineering
University of Wisconsin-Madison

Wisconsin Electric Machines and Power Electronics Consortium

RESEARCH REPORT
93-24

Electromagnetic Model for Evaluation of Flux Harmonics and Resulting Vibrations in Induction Machines

A.A. Fahim and T.A. Lipo
Dept. of Electrical and Computer Engineering
University of Wisconsin-Madison
1415 Johnson Drive
Madison, WI 53706

C.J. Slavic
General Electric Co.
Schenectady, NY

WEMPEC

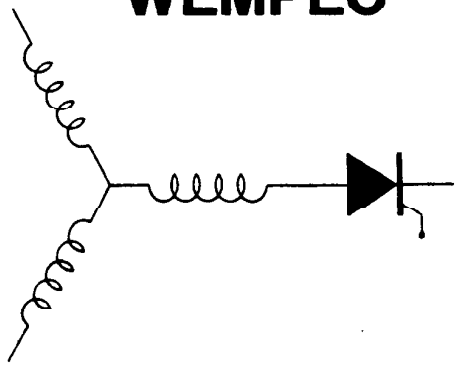

Department of Electrical and Computer Engineering
1415 Johnson Drive
Madison, Wisconsin 53706

ELECTROMAGNETIC MODEL FOR EVALUATION OF FLUX HARMONICS AND RESULTING VIBRATIONS IN INDUCTION MOTORS.

A. A. Fahim
University of Wisconsin-Madison U.S.A.

T. A. Lipo
University of Wisconsin-Madison U.S.A.

C. J. Slavic
General Electric Co. Schenectady, NY U.S.A.

Abstract

An electromagnetic field approach for accurate determination of the amplitudes and the frequencies of the harmonic components of the field generated within induction motors and the associated torsional and radial vibrations is given. The relative motion of the slotted boundaries as well as the rotor induced current are taken into consideration. A novel approach based on matrix methods is introduced to solve the coupled equations of the harmonic components. Attention has been focused on the process by which the harmonics of the radial and the tangential flux components interact to produce the harmonic forces. Display of the flux and the force harmonic spectra is provided which clearly shows the contribution of each harmonic component to the vibrating forces.

INTRODUCTION

It has always been the aim of engineers to design electrical machines with low levels of vibration and audible noise. This is particularly important in certain applications for which noise is undesirable. Vibrations result from the oscillating forces generated by the electromagnetic field harmonics within the machine. Complete elimination of all field harmonics is clearly impossible, since harmonics are inherent in the physical structure of the machine itself. However, canceling certain harmonic components, for example those corresponding to certain mechanical resonances, or reducing their level can possibly be achieved by appropriate modifications of the geometrical structure or the excitation current. Accurate determination of the amplitudes and the frequencies of the generated harmonic field within the machine and the associated torsional and radial vibrations will be the first step in reducing, or even canceling, certain harmonics, and thus designing a "quiet" machine.

The earliest work on this problem was mainly carried out using the concepts of mmf and permeance waves. This form of analysis is essentially one dimensional, with only the radial component of the field considered. A two-dimensional solution has been attempted using conformal transformation and finite elements techniques. However for squirrel cage induction machines an accurate representation of the rotor induced current presents difficulties in both methods.

In the present work a new approach utilizing electromagnetic field analysis of electrical machines is introduced based on expansion of the periodic slotted structures of both the stator and rotor in terms of spatial, or spatial and temporal, harmonic components of various orders. Maxwell's equations are used to represent the resultant electromagnetic field generated by the stator excitation and the rotor induced current in terms of spatial and temporal harmonic components. While this spectral representation is similar to that introduced by Binns [1] - [5], this approach is capable of determining the amplitudes as well as frequencies of the harmonic components. By applying the appropriate boundary conditions at the surfaces separating the different regions of the machine a set of algebraic equations that couple the field harmonic components is obtained. These equations are solved using a novel approach based on matrix methods. Solution of the final matrix equation provides the amplitudes and the frequencies of all field harmonics. The force components and their spatial and temporal harmonics can be easily determined and the effect of the machine physical structure and dimensions on the spectral components of the force distribution assessed.

ELECTROMAGNETIC FIELD MODEL

To investigate the generated flux due to both stator excitation and rotor induced currents, a two dimensional field model representing the most general induction motor configuration is shown in Fig. 1. The r-θ cross sectional plan of the whole motor region is divided into subregions as shown. To determine the harmonics due to stator and rotor slots and the rotor relative motion, the following assumptions are made:

(1) The stator winding is replaced by an equivalent current sheet. For a three-phase machine the general expression for the stator excitation current density is:

$$J_s(\theta,t) = \sum_{m,n} J_s(n,m)\, e^{jnp\theta}\, e^{jm\omega_o t} \qquad (1)$$

where ω_o is the supply frequency, θ is the angle subtended at the center of the machine (in mechanical degrees) and p is the number of pole pairs. $J_s(n,m)$ is the amplitude of the spatial harmonic of order n, which is determined by the winding distribution function, and the temporal harmonic of order m, which is determined by the nature of the excitation current. In this work it is assumed that the winding is a sinusoidally distributed balanced three-phase winding, so that n and m take only the value 1. The amplitude of the fundamental component of the excitation current is determined from the winding distribution function.

(2) The stator slots are replaced by a region of thickness equal to the slot depth. This region has a periodic permeability function $\mu(\theta)$.

(3) The rotor slots are replaced by a layer on the top of the rotor back iron region. This layer has a thickness equal to the rotor slot depth and a periodic conductivity function $\sigma(\theta,t)$ that is also a function of time since the rotor rotates with speed ω_m and conductivity $\sigma(\theta,t)$

The periodic permeability $\mu(\theta)$ and conductivity $\sigma(\theta,t)$ functions can be expressed in terms of Fourier series:

$$\mu(\theta) = \sum_n b(n)\, e^{jnN_s\theta} \qquad (2)$$

$$\sigma(\theta,t) = \sum_n a(n)\, e^{jnN_r\theta}\, e^{jnN_r\omega_m t} \qquad (3)$$

Here, the number of stator slots, N_s, determines the periodicity of $\mu(\theta)$; the number of rotor slots, N_r, determines the angular periodicity of $\sigma(\theta,t)$ and the rotor mechanical speed, ω_m, determines its temporal periodicity. The amplitudes of the harmonic components $b(n)$ and $a(n)$ are obtained for a rectangular shape slots as:

$$a(n) = \sigma \frac{w_r}{p_r} \frac{\sin n\pi \frac{w_r}{p_r}}{n\pi \frac{w_r}{p_r}} \qquad (n\neq 0)$$
$$a(0) = \sigma \frac{w_r}{p_r} \qquad (4)$$

$$b(n) = (\mu_i - \mu_o) \frac{t_s}{p_s} \frac{\sin n\pi \frac{t_s}{p_s}}{n\pi \frac{t_s}{p_s}} \qquad (n\neq 0)$$
$$b(0) = (\mu_i - \mu_o) \frac{t_s}{p_s} \qquad (5)$$

where W is the slot width, t is the tooth width, p_x is the pitch and the subscript x=s and x=r refers to stator and rotor respectively.

ELECTROMAGNETIC FIELD EQUATIONS

From Maxwell's equations, the general differential equation describing the axial component of the magnetic vector potential $\mathcal{A}$ in the different regions of the motor is the Helmholtz equation:

$$\nabla^2 \mathcal{A} = \mu [J_s + J_e] \qquad (6)$$

where J_s is the stator excitation surface current density and J_e is the rotor induced current density, which is related to $\mathcal{A}$ by:

$$J_e = -\sigma \left[\frac{\partial \mathcal{A}}{\partial t} + \omega_m \frac{\partial \mathcal{A}}{\partial \theta} \right] \qquad (7)$$

From Eqs. 6 and 7, it can be conjectured that $\mathcal{A}$ will contain harmonic components of the same temporal and spatial frequencies as $J_s(\theta,t)$, $\mu(\theta)$ and $\sigma(\theta,t)$, so that $\mathcal{A}$ may generally be written in the form:

$$\mathcal{A}_i(\theta,t)=\sum_{m,l} A_i(m,l)\, e^{j(mN_r+lN_s+p)\theta}\, e^{j(mN_r\omega_m+\omega_o)t} \qquad (8)$$

The index i=1,2,3,4 is used to denote the different regions within the motor. The indexes m and l represent the effects of the harmonics of the rotor and stator slotted structures, respectively. They contribute to an electromagnetic field with spatial frequency (mN_r+lN_s+p), or effective number of poles, and temporal frequency $(mN_r\omega_m+\omega_o)$. The amplitude $A_i(m,l)$ is a function of the radial distance r within region i. For the Helmholtz equation to be satisfied, these amplitudes must have the following dependence on r:

$$A_i(m,l) = C_i(m,l)\, r^{M(m,l)} + D_i(m,l)\, r^{-M(m,l)} \qquad (9)$$

where $M(m,l)=|mN_r+lN_s+p|$ and the constants $C_i(m,l)$ and $D_i(m,l)$ are to be determined from the boundary conditions at the three surfaces separating the four regions.(Fig. 1) as well as at r=0 and r=∞. The continuity of the normal components of the magnetic flux density B_r and the discontinuity of the tangential components of the magnetic field intensity H_θ at the surfaces r= r_a, r_{s1} and r_{s2} result in six equations relating the values of $\mathcal{A}i$(i=1,2,3,4), the parameters of the four regions and the excitation and the induced current sheets. Substituting for $\mathcal{A}_1$, $\mathcal{A}_2$, $\mathcal{A}_3$, $\mathcal{A}_4$, and J_e using Eqs. (7-8), and equating each of the harmonics of the same order on both sides of the boundary conditions, six equations relating the six unknown amplitudes C1, C2, D2, C3, D3, D4 are obtained. By a series of substitutions they can be reduced to a single equation relating the amplitudes of the harmonic components of $C1(m,l)$:

$$[C1(m,l)\, y_1(m,l)] + \left[\sum_{n_2} C1(m-n_2,l)\, y_2(m,l,n_2)\right] + \left[\sum_{n_3} C1(m,l-n_3)\, y_3(m,l,n_3)\right] + \left[\sum_{n_2}\sum_{n_3} C1(m-n_2,l-n_3)\, y_4(m,l,n_2,n_3)\right] + \left[\sum_{n_3}\sum_{n_4} C1(m,l-n_3-n_4)\, y_5(m,l,n_3,n_4)\right] + \left[\sum_{n_2}\sum_{n_3}\sum_{n_4} C1(m-n_2,l-n_3-n_4)\, y_6(m,l,n_2,n_3,n_4)\right] = F(m,l) \qquad (10)$$

The functions y_1-y_6 and F are defined in terms of the machine main dimensions, parameters and the stator excitation current, see Appendix (I).

Finally to solve Eq. 10 for $C1(m,l)$ the summation terms are cast in the matrix form :

$$\sum_{n'} Y(n',n)\, C1(n') = F(n) \qquad (11)$$

where $Y(n,n')$ and $F(n)$ are known elements of matrices described in Appendix(I) and $C1(n')$ are elements of a column matrix that is simply a stacking of the variables {[$C1(m,l)$, l = ±1,±2,±3,...], m=±1,±2,±3,....}.

This matrix equation can be solved for the unknowns $C1(n')$, from which the amplitudes $C1(m,l)$ of the different harmonic components are obtained. Once $C1(m,l)$ are determined, the other amplitudes can be computed by use of the boundary condition relations and thus the magnetic vector potential $\mathcal{A}$ can be determined in all regions of the motor.

Flux density distribution

Knowing the magnetic vector potential distribution within motor different regions, $\mathcal{A}_1$, $\mathcal{A}_2$, $\mathcal{A}_3$ and $\mathcal{A}_4$, the two components of the magnetic flux density $\mathcal{B}_r$ and $\mathcal{B}_\theta$ are defined everywhere in the defined space by:

$$\mathcal{B}_r = \frac{1}{r}\frac{\partial \mathcal{A}}{\partial \theta} \qquad \mathcal{B}_\theta = -\frac{\partial \mathcal{A}}{\partial r} \qquad (12)$$

Generally $\mathcal{B}_r$ and $\mathcal{B}_\theta$ can be written in the form:

$$\mathcal{B}(\theta,t) = \sum_{m,l} B_r(m,l)\, e^{j(mN_r+lN_s+p)}\, e^{j(mN_r\omega_m+\omega_o)t} \qquad (13)$$

$$\mathcal{B}_\theta(\theta,t) = \sum_{m,l} B_\theta(m,l)\, e^{j(mN_r+lN_s+p)}\, e^{j(mN_r\omega_m+\omega_o)t} \qquad (14)$$

For $r=r_{s1}$ (the stator surface) the amplitudes of the harmonics of the radial and the tangential field components are:

$$B_r(m,l) = \sum_{m,l} \frac{j}{r_{s1}} (mN_r + lN_s + p)) \; .$$

$$\left[C2(m,l)\, r_{s1}^{M} + D2(m,l) r_{s1}^{-M} \right] \qquad (15)$$

$$B_\theta(m,l) = \sum_{m,l} - M\left[C2(m,l)\, r_{s1}^{M-1} + D2(m,l)\, r_{s1}^{M-1} \right] \qquad (16)$$

Knowing the amplitudes $B(m,l)$ and the space and the time frequencies of each harmonic component, complete information about the air gap flux harmonic contamination is obtained.

Force distribution along stator surface

Knowing the two components of the magnetic flux density $\mathcal{B}_r$ and $\mathcal{B}_\theta$ at the stator surface ($r=r_{s1}$), the radial and the tangential magnetic force density distributions are obtained using of Maxwell's stress formula,

$$F_r = \frac{\mathcal{B}_r^2 - \mathcal{B}_\theta^2}{2\mu_o} \qquad F_\theta = \frac{\mathcal{B}_r\, \mathcal{B}_\theta}{\mu_o} \qquad (17)$$

Substituting for $\mathcal{B}_\theta$ and $\mathcal{B}_r$ using Eqs. 13,14, the Fourier series expression for the tangential force F_θ is :

$$\overline{F}_\theta(\theta,t) = \frac{0.5}{\mu_0} \mathrm{Real} \sum_m e^{j(mN_r\omega_m)t} \sum_l e^{j(mN_r + lN_s)\theta}$$

$$\sum_{m_1,l_1} B_\theta(m_1,l_1)\, B_r^*(m_1-m, l_1-l) \qquad (18)$$

Similarly the radial force density is:

$$\overline{F}_r(\theta,t) = \frac{0.25}{\mu_0} \mathrm{Real} \sum_m e^{j(mN_r\omega_m)t} \sum_l e^{j(mN_r + lN_s)\theta}$$

$$\sum_{m_1,l_1} B_r(m_1,l_1) B_r^*(m_1-m,l_1-l) - B_\theta(m_1,l_1) B_\theta^*(m_1-m,l_1-l) \qquad (19)$$

where B_r^* and B_θ^* are the complex conjugates of B_r and B_θ.

MODEL FOR CALCULATIONS

As an example of the capability of this approach to provide a wide range of information, the amplitudes and the frequencies of the generated harmonics can be computed for both the radial and the tangential flux and force components. The flux and the forces spectra as well as their distributions can be plotted along any radial surface within the machine. The theory developed in this work, has been applied to a typical 3-phase, 4-pole cage motor with a stator and rotor slot number of 48 and 37 respectively. The spatial frequency spectra of the radial flux at the rotor surface is shown in Fig. 2, while the temporal distribution is shown in Fig. 3. Good agreement of the waveforms with those of previous researchers is in evidence [1-5]. The spatial harmonic spectrum is shown for the tangential flux component at the rotor surface in Fig. 4 and for the temporal distribution in Fig. 5. An important capability of this approach is the ability of predict not only the frequency of the force components but also their amplitudes. The temporal distribution of the radial and the tangential force components at the stator surface are shown in Figs. 6 and 7 respectively.

CONCLUSIONS

An analytical technique has been developed for determining the frequencies and amplitudes of the spatial and temporal harmonic components of the electromagnetic field in induction motors, and their associated torsional and radial forces. The relative strengths of these harmonics are sensitive to the geometry. The technique can be used to facilitate the design of machines with reduced vibrations.

REFERENCES

[1] Binns, K.J. and G. Rowlands-Rees, "Simple rules for the elimination of cogging torque in squirrel cage induction motors". Proc. IEE. Vol. 121, No. 1, Jan. 1974.

[2] Binns, K.J. and E. Schmid, "Some concepts involved in the analysis of the magnetic fields in cage induction machines". Proc. IEE. Vol. 122, No. 2, Feb. 1975.

[3] Binns, K.J. and G. Rowlands-Rees, "Main flux pulsation & tangential tooth ripple forces in induction motors". IEE. Vol. 122 No. 3, March 1975.

[4] Binns, K.J. and G. Rowlands-Rees, "Radial tooth ripple forces in induction motors due to the main flux". Proc. IEE. Vol. 125, No. 11, Nov. 1978.

[5] Binns, K.J. and P.A. Kahan, "Effect of load on the tangential force pulsations and harmonic torques of squirrel cage induction motors", Proc. IEE, Vol. 128, Pt. B, No. 4, July 1982.

APPENDIX I

As an example of the y and the F functions in Eq. 10

$$y_2(m,l,n_2)=\left[0.5j\omega\mu_o\Delta r_a a(n_2)\gamma(m-n_2,l)\frac{r_a}{M}r_a^{M_2-M}\right]\left[0.5\left(1-\left(\frac{r_a}{r_{s1}}\right)^{2M}\right)\left(1+\left(\frac{r_{s1}}{r_{s2}}\right)^{2M}\right)-\left(\frac{r_{s1}}{r_{s2}}\right)^{2M}+\left(\frac{r_a}{r_{s2}}\right)^{2M}\right]$$

$$y_3(m,l,n_3)=-\left[\frac{b(n_3)}{\mu_o}\frac{M_3}{M}r_{s1}^{M_3-M}\left(\frac{r_a}{r_{s1}}\right)^{2M_3}\left(1+\left(\frac{r_{s1}}{r_{s2}}\right)^{2M}\right)\right]+\left[\frac{b(n_3)}{\mu_i}\frac{M_3}{M}r_a^{M_3}r_{s2}^{-M}\left(\frac{r_a}{r_{s2}}\right)^{M_3}\right]$$

$$F(m,l)=J_s(1)\,\Delta r_s\,\delta(m)\frac{r_{s1}}{M}\left[b(l)\,r_{s1}^{M}+b(l-n_3)\frac{b(n_3)}{\mu_i}r_{s2}^{M}\sum_{n_3}\left(\frac{r_{s2}}{r_{s1}}\right)^{M_3}\left(1-\left(\frac{r_{s1}}{r_{s2}}\right)^{2M_3}\right)\right]$$

where

$$M_2=\ M(m-n,l)=|(m-n)N_r+lN_s+p|$$
$$M_3=\ M(m,l-n)=|(m)N_r+(l-n)N_s+p|$$

APPENDIX II

To write Eq. 10 in the general matrix form (Eq. 11), the six terms of the equation can be rewritten as follows:

The 1st. term

$$C(m,l)\,y_1(m,l)=\sum_{m',l'}C(m-m',l-l')\,y_1(m,l)\,\delta(m')\,\delta(l')$$

The 2nd term

$$\sum_{n_2}C(m-n_2,l)y_2(m,l,n_2)=$$

$$\sum_{m',l'}C(m-m',l-l')y_2(m,l,m')\delta(l')$$

The 3rd term

$$\sum_{n_3 l}C(m,l-n_3)y_3(m,l,n_2)=$$

$$\sum_{m',l'}C(m-m',l-l')\,y_3(m,l,l')\,\delta(m')$$

The 4th term

$$\sum_{n_2}\sum_{n_3}C(m-n_2,l-n_3)\,y_4(m,l,n_2,n_3)=$$

$$\sum_{m',l'}C(m-m',l-l')\,y_4(m,l,m',l')$$

The 5th term

$$\sum_{n_3}\sum_{n_4}C(m,l-n_3-n_4)\,y_5(m,l,n_3,n_4)=$$

$$\sum_{m',l'}C(m-m',l-l')\sum_{n_4}y_5(m,l,l'-n_4,n_4)\,\delta(m')$$

The 6th term

$$\sum_{n_2}\sum_{n_3}\sum_{n_4}C(m-n_2,l-n_3-n_4)\,y_6(m,l,n_2,n_3,n_4)=$$

$$\sum_{m',l'}C(m-m',l-l')\sum_{n_4}y_6(m,l,m',l'-n_4,n_4)$$

where the δ function is defined as:

$$\delta(m)=0 \qquad m\neq 0$$

$$\delta(0)=1$$

Adding the terms 1 to 6, Eq. 10 is converted to the form:

$$\sum_{m',l'}C(m-m',l-l')\,Y(m,l,m',l')=F(m,l)$$

Relating the double array arguments $m-m'$, $l-l'$ to a single argument n' and m, l to n, the above equation can be rewritten as Eq. 11.

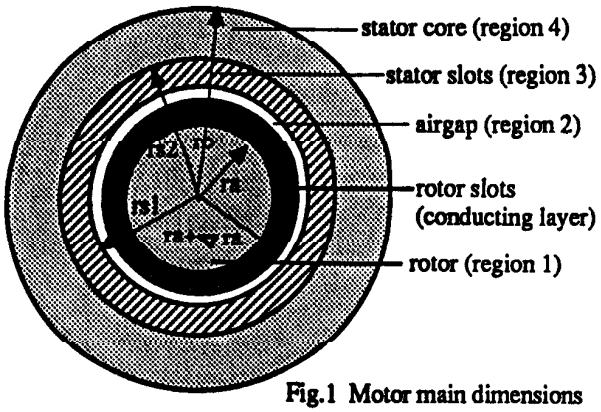

Fig.1 Motor main dimensions

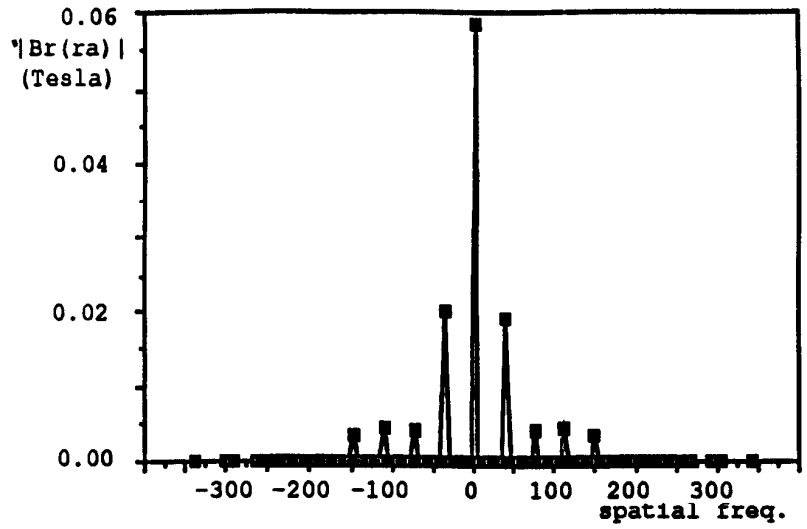

Fig.2 Spatial harmonic spectrum of the radial flux density.

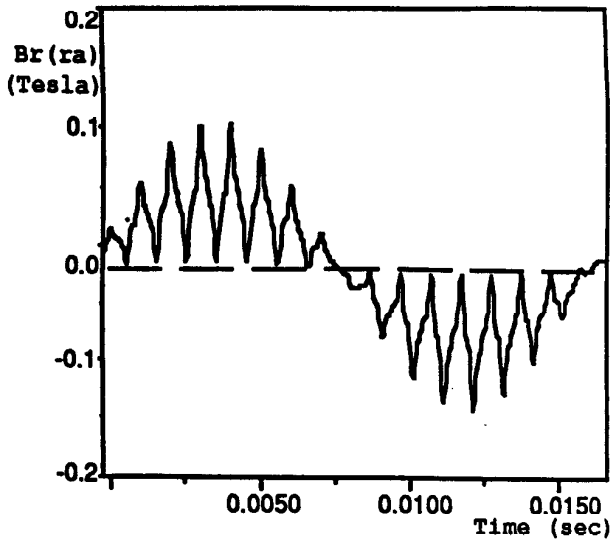

Fig.3 Temporal distribution of the radial flux density.

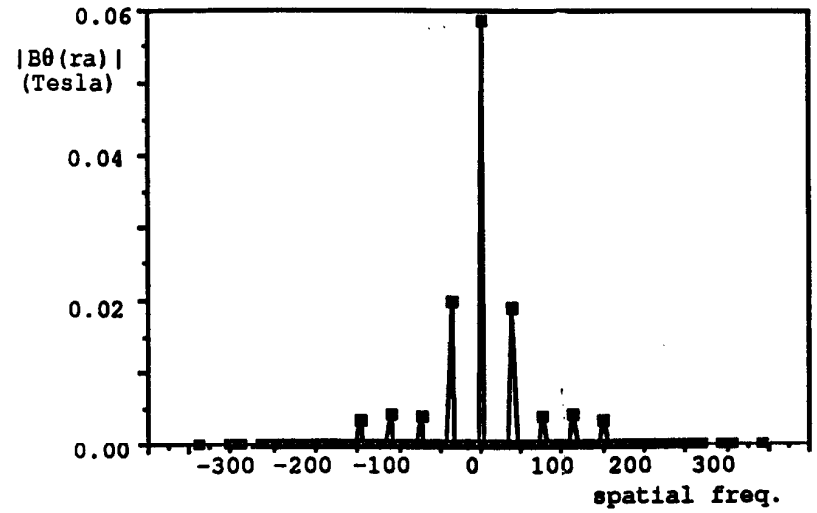

Fig.4 Spatial harmonic spectrum of the tangential flux density.

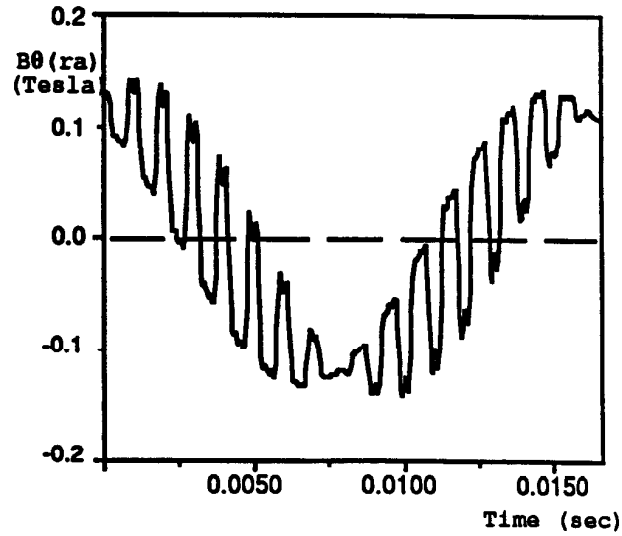

Fig.5 Temporal distribution of the tangential flux density.

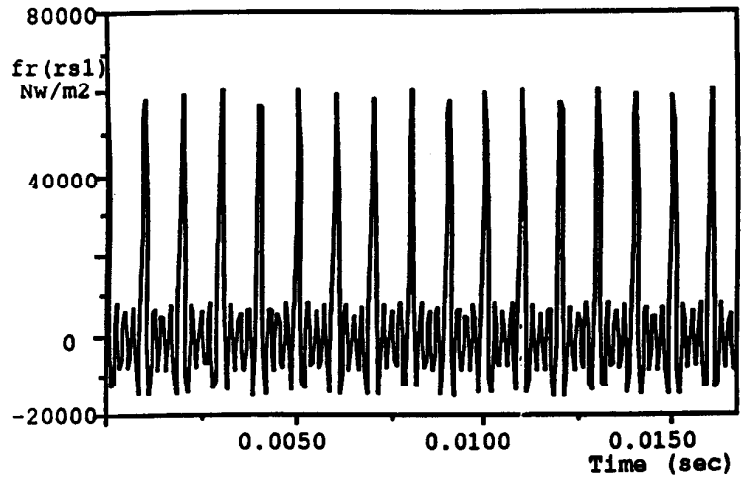

Fig.6 Temporal distribution of the radial force density at stator surface.

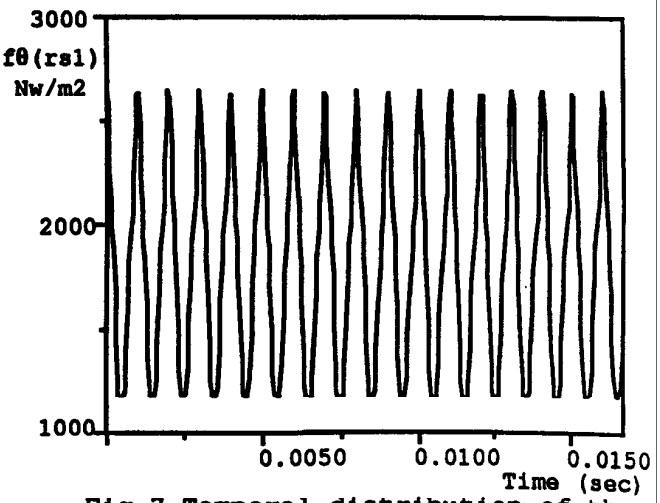

Fig.7 Temporal distribution of the tangential force density at stator surface.